

DESIGN OF THE MAGNETIC FIELD FOR THE MILAN SUPERCONDUCTING CYCLOTRON

G. Bellomo , C. De Martinis , L. Serafini

University of Milan and Istituto Nazionale di Fisica Nucleare , Milan , ITALY

Abstract.- A detailed presentation of the magnetic field properties of the machine is given. The anticipated operating conditions and the resulting beam dynamics properties are also discussed.

1. Introduction.- The main characteristics of the magnetic field for the K-800 Milan Superconducting Cyclotron have been analyzed to verify that the expected performances of the machine can be met. Acceleration of fully stripped light ions up to 100 MeV/n and a wide dynamic range, with a 22 kgauss field low limit are anticipated. The overall iron geometry is described elsewhere¹⁾. This paper will present the results of field trimming calculations and the most relevant equilibrium orbit properties.

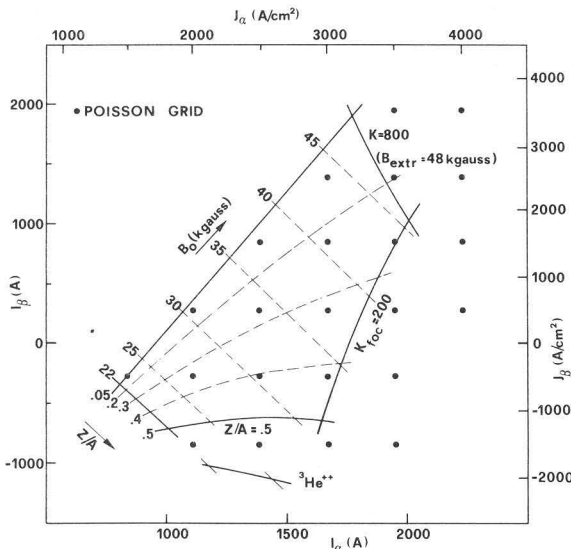


Fig.1 - Operating diagram of the machine in the (I_α, I_β) plane. Also indicated are the constant B_0 and Z/A lines. The dots mark the points of Poisson calculations.

2. General characteristics of the magnetic field.- The average field produced by the iron, $\bar{B}_{iron}(r, I_\alpha, I_\beta)$, was computed with the code Poisson, together with the model described in ref.1. Poisson computations were carried out at 23 (I_α, I_β) values, shown by the dots in fig.1. This grid covers the machine operating range for the interpolation of $\bar{B}_{iron}(r, I_\alpha, I_\beta)$ at any intermediate value of (I_α, I_β) . The bending and focusing limits, corresponding to a $K=800$ and $K_{foc}=200$, together with $Z/A=.5$ and $Z/A=.05$ lines are the boundaries of the operating diagram. The $Z/A=.67$ line corresponding to different center field levels for the ${}^3\text{He}^{++}$ ions is also plotted.

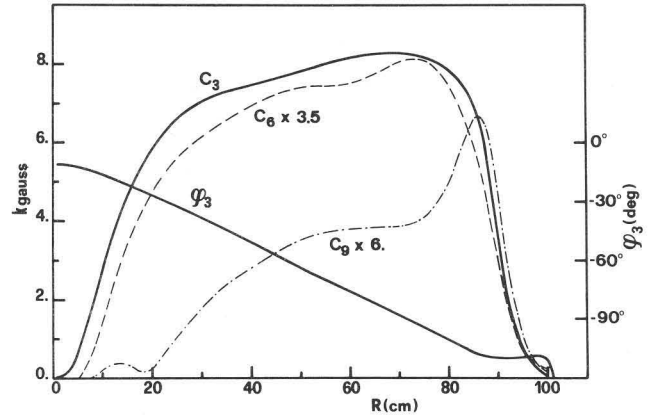


Fig.2 - 3rd harmonic amplitude and phase (solid lines). 6th (dashed line) and 9th (dashed-dotted line) harmonic amplitudes are multiplied by the indicated factors.

The azimuthal modulation produced by the pole tip geometry was calculated according to the full saturation hypothesis of the pole tip surface, with a uniform magnetization of $M=2.14$ T directed along the z -axis²⁾. The amplitude and phase of the 3rd field harmonic, with the 6th and 9th harmonic amplitudes are plotted in fig.2.

The field modulation is kept constant with respect to (I_α, I_β) in all the calculations, while the variations of $\bar{B}_{iron}(r, I_\alpha, I_\beta)$ with the main coils excitation is entirely taken into account by the Poisson calculations. At a current density of $J_\alpha=3000$ A/cm² and $J_\beta=-1500$ A/cm², close to the one needed for fully stripped light ions at 100 MeV/n, the calculated average iron field is given by the solid line of fig.3. Also plotted, dashed line, is the theoretical best field needed to minimize the trim coil power requirements, computed according to the method described in ref.3. The agreement, up to $r=84$ cm which is the last radius used in the isochronous field fitting, is excellent. A maximum difference of ± 20 gauss is observed, well within the uncertainties of the \bar{B}_{iron} computations.

At the innermost radii, $r \leq 14$ cm, the average iron field presents a central cone which has been added for the use of the machine with an internal ion source. This cone field is produced by the dashed iron shims indicated in the left part of fig.4, added to the circular and hill part of the plug. Without these auxiliary shims one would obtain an average field equal to the theoretical best field. To adjust the shape and the level of the cone field a small coil is inserted in the plug.

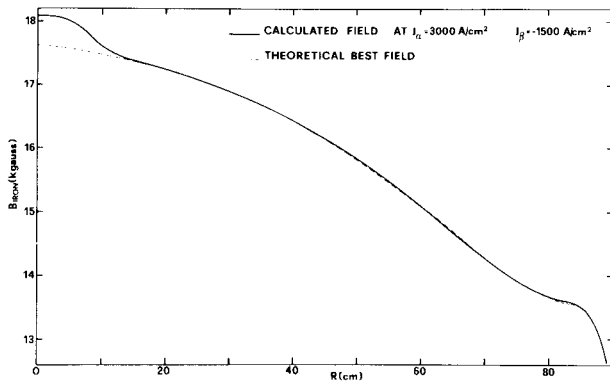


Fig. 3 - Average field produced by the iron (solid line) compared with the theoretical best field (dashed line). See text for details.

Having a 3.7 cm inner radius, 5 cm outer radius and 3 cm height, at a minimum distance of 5 cm from the median plane, it produces an air core field as shown in fig. 4.

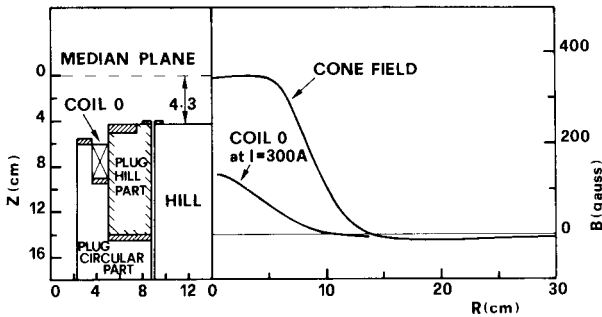


Fig. 4 - On the left: plug and hill central region radial profile. The dashed shims produce the iron cone field shown on the right. The air core field at 300 A for the coil 0, inserted in the plug, is also plotted.

3. Field trimming. - To properly shape the total average field $\bar{B}_{tot}(r, I_\alpha, I_\beta) = \bar{B}_{iron}(r, I_\alpha, I_\beta) + B_{coils}(r, I_\alpha, I_\beta)$ and fulfil the isochronism requirement, twenty trim coils, wound around the hill upper part¹⁾, are available. Their form factors can be seen in fig. 5 at an excitation of 300 A, with the radial position on the hill shown at the bottom.

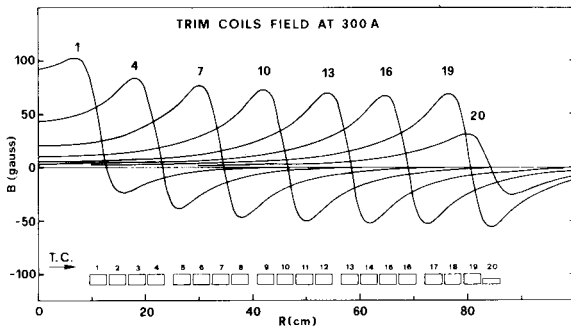


Fig. 5 - Air core average field at 300 A for the indicated trim coils. The geometry of all the twenty trim coils is also shown at the bottom.

The results of the isochronous field fittings, carried out via a least squares procedure are so far quite good. Isochronism is obtained over the entire operating diagram with rather low trim coil powers. The latter

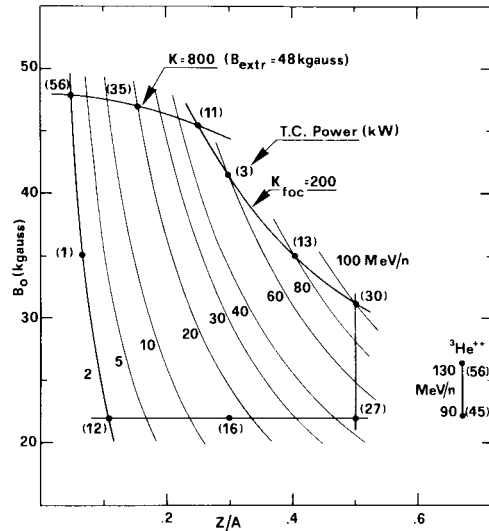


Fig. 6 - Operating diagram of the machine in the $(B_0, Z/A)$ plane with the lines of constant energy per nucleon and the trim coil power needed to achieve isochronism.

are presented in fig. 6 for ten representative ions along the contour of the operating diagram and two representative cases for ${}^3\text{He}^{++}$. The fitting procedure has been carried out by fixing a maximum current of 400 A for every trim coil and a very precise isochronous field has nevertheless been obtained for all cases ($\Delta B/B \leq 0.1\%$).

4. Equilibrium orbit properties. - The total average field resulting from the fitting procedure, together with the axial focusing frequency and phase are presented in figs. 7 and 8, as a function of the E.O. radius, for two pairs of representative ions. One corresponds to the fully stripped light ions for the highest (31.3 kgauss) and the lowest (22 kgauss) center field level.

The minimum ν_z value reached is about .18 for the 100 MeV/n case, implying a fairly large margin in axial focusing. The oscillations in the ν_z curves due to the field gradients produced by the trim coils are quite small, as expected by the low power levels. The phase curves show the effect of the central cone field and of the acceleration above isochronism ($\phi_{min} \approx -35^\circ$) before the extraction radius. The latter is carried out in order to increase the axial focusing in the high field gradient region. Extraction takes place, however, at a maximum positive phase of $+35^\circ$ for the most energetic ions.

The anticipated radial cut of the sectors at the outermost radii seems sufficient in lowering the ν_z for the lowest center field levels, thus avoiding an excessive inward movement of the $\nu_r + 2\nu_z = 3$ resonance¹⁾.

5. Influence of trim coils on E.O. properties. - The trim coils excitation produces both the average field needed for fitting the isochronous field and an azimuthal modulation due to the geometry of the trim coils themselves. The resulting trim coil modulation for example adds a 3rd harmonic amplitude $C_3^{tc}(r) \leq 80$ gauss for the case of the 100 MeV/n ions. A perturbative effect $\delta C_1(r)$, of the same order as $C_1^{tc}(r)$, is thus produced on the $C_1(r)$ plotted in fig. 2 ($\delta C_1(r)/C_1(r) \leq 1.5\%$). This causes the isochronous field $B_{isoc}(r)$, which is a function of $C_1(r)$ and their derivatives⁴⁾, to be perturbed

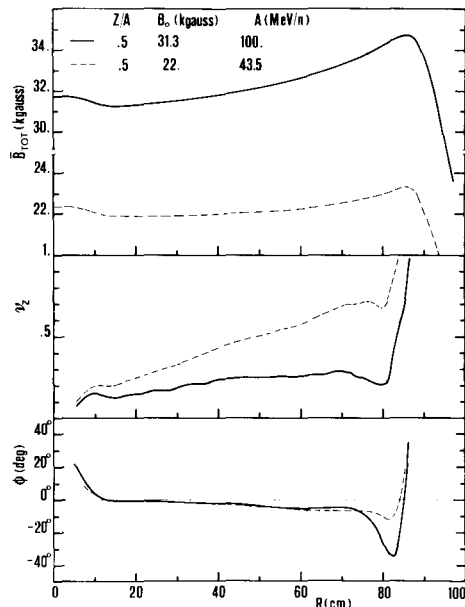


Fig.7 - Average total field, ν_z and phase, as a function of the radius, for an ion with $Z/A=0.5$ and a center field level of 22. and 31.3 kgauss.

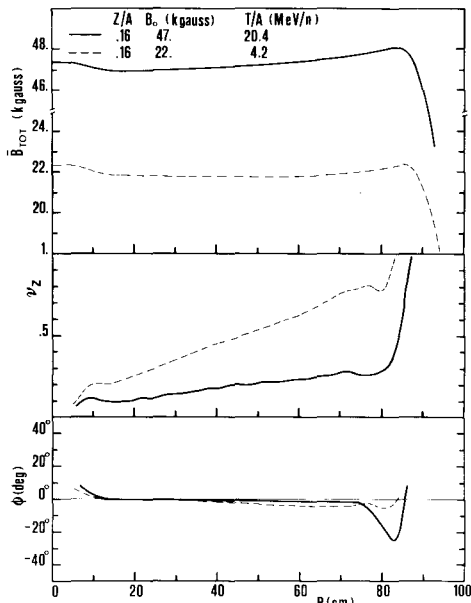


Fig.8 - Average total field, ν_z and phase, as a function of the radius, for an ion with $Z/A=0.16$ and a center field level of 22. and 47. kgauss.

too. Let $B_{isoc}^*(r)$ be this perturbed isochronous field; then a new set of trim coil currents will be needed to fit $B_{isoc}^*(r)$, therefore producing a new $\delta C_1(r)$ perturbation which may be different. An iterative procedure is thus needed. The iteration is stopped when the difference $\delta B_{isoc}^*(r) = B_{isoc}^{*n+1}(r) - B_{isoc}^{*n}(r)$ between the perturbed isochronous fields in two successive cycles is .002% of the $B_{isoc}^{*n}(r)$ for all the r values. The final field map is obtained by fitting the $B_{isoc}^*(r)$ of the last cycle and adding to the total average field so produced both the iron modulation map and the modulation map produced

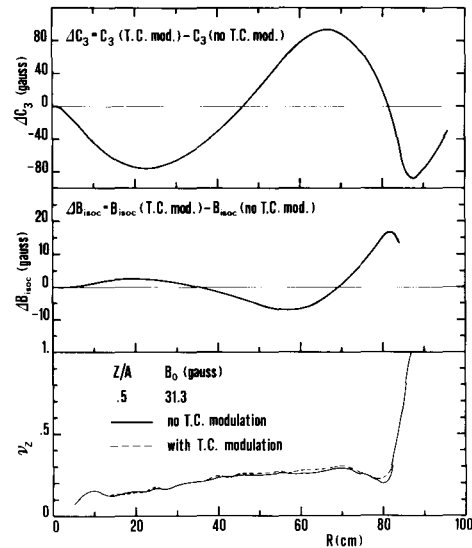


Fig.9 - Perturbation on the 3rd harmonic amplitude produced by the trim coils (ΔC_3) and consequent variation of the isochronous field (ΔB_{isoc}). On the bottom ν_z calculated with the trim coil modulation (dashed line) and without (solid line). See text for details.

by the trim coils at the currents needed for fitting $B_{isoc}^*(r)$.

In fig.9 the results of such an iterative calculations for the 100 MeV/n ions can be seen. The difference $\Delta C_3(r)$ between the 3rd harmonic amplitude for the final field map (with the trim coil modulation) and the unperturbed $C_3(r)$ is shown, as a function of the radius, in the upper part of the figure. The central part presents the difference $\Delta B_{isoc}(r)$ between the perturbed $B_{isoc}^*(r)$ computed at the last cycle and the unperturbed $B_{isoc}(r)$. $\Delta B_{isoc}(r)$ thus represents the perturbation generated by the trim coils on the isochronous field: it is more pronounced, roughly speaking, where the derivative of the 3rd harmonic perturbation, $\Delta C_3(r)$, is larger with respect to the derivative of the unperturbed $C_3(r)$.

The effect of such a perturbation on the axial focusing are shown in the lower part by the two ν_z curves corresponding to the final field map with the trim coil modulation (dashed line) and to the unperturbed field map without the trim coil modulation (solid line). Since the trim coil field contributions are positive for this case from $r=44$ cm to $r=82$ cm, in this region the trim coil modulation adds to the iron modulation, increasing the flutter. This accounts for the small growth of ν_z in the indicated region, while the more pronounced oscillations of ν_z are due to the local harmonic gradients produced by the trim coils. Nevertheless, also for the present case in which the trim coil field contribution is quite large, as the power requirement, the effects of the trim coil modulation are, although visible, rather small.

References

1. E.ACERBI et al., The Milan Superconducting Cyclotron project, paper presented to this conference
2. M.M.GORDON et al., Particle Accelerators 10 (1980)217
3. G.BELLOMO et al., IEEE Trans. NS-26 (1979) 2095
4. M.M.GORDON et al., ORNL-2765 (1959)